Measurement of elastic cross section for cold cesium collisions

S. A. Hopkins, S. Webster, J. Arlt, P. Bance, S. Cornish, O. Maragò, and C. J. Foot
Clarendon Laboratory, Department of Physics, University of Oxford, Parks Road, Oxford OX1 3PU, United Kingdom
(Received 26 March 1999; published 11 February 2000)

We have measured the time taken for a magnetically trapped cloud of cold cesium atoms in the $(F=3,m_F=-3)$ ground state to rethermalize from a nonequilibrium spatial and velocity distribution. From these measurements we infer the dependences of the elastic scattering cross section on temperature and magnetic field in the ranges $1-30$ μK and 0.05–2.0 mT, respectively. We determine a lower bound on the magnitude of the $(3,-3)+(3,-3)$ *s*-wave scattering length of $940a_0$.

PACS number(s): 34.50.Pi, 03.75.Fi, 05.30.Jp, 32.80.Pj

The first observations of Bose-Einstein condensation (BEC) in dilute alkali-metal gases in 1995 spawned a rapid growth of interest in BEC, including attempts to extend the number of different condensed isotopes beyond the first three: ^{87}Rb, ^{23}Na, and ^{7}Li [1–3]. Spin-polarized hydrogen^{1}H was added to the fold in 1998 [4], and attempts are currently under way to condense ^{85}Rb, K, Cs, metastable He^+, Cr and molecules. The study of cold atomic collisions is highly relevant to the field of BEC because the evaporative cooling technique used to reach quantum degeneracy depends critically upon favorable rates of elastic and inelastic collisions [19]. In the case of cesium the collisional properties of cold atoms also affect the use of the element in atomic fountain time standards and there has been considerable experimental [5–12] and theoretical work [13–17].

Initial attempts to condense cesium, by groups at ENS in Paris [6,7] and at Oxford [8,9], concentrated on the spin-polarized $(F=4,m_F=+4)$ state and showed that, in the regime of pure *s*-wave collisions, the elastic cross section of the $(4,+4)$ state varied inversely with temperature, which is indicative of a zero energy resonance [6,18]. The experiments also revealed a high inelastic collision rate, which ruled out the possibility of observing BEC. The experimental effort then shifted to the $(F=3,m_F=-3)$ state, where the inelastic rates were found to be lower, allowing the observation of runaway evaporative cooling [19] up to phase space densities $\sim 10^{-2}$ [8,10]. However, the rate of inelastic collisions was still too high, preventing the achievement of BEC in Cs thus far. The high inelastic rates had not been predicted by theoretical models, and improved calculations of cold collisional rates in Cs have been made [15–17]. However, such calculations are difficult owing to the limited amount of experimental data available and the impossibility of *a priori* calculations for an element as heavy as cesium. It has been suggested that a favorable ratio of elastic to inelastic collisions in the $(3,-3)$ state which would allow evaporative cooling to BEC, might be found at very low bias fields ($\leqslant 0.05$ mT [11,20]) because the *d*-wave centrifugal barrier in the outgoing channel suppresses the inelastic process when the Zeeman energy released is less than the barrier height. Alternatively, since the inelastic rate varies strongly with magnetic field due to Feshbach resonances, observed recently for the $(3,-3)$ state in the inelastic rate at 3.1 and 3.4 mT [12], there may be a value of field which gives a favorable ratio of good to bad collisions [15,20,21]. Feshbach resonances have also been recently seen in work on ^{23}Na [22] and ^{85}Rb [23] at high fields and are important as they enable magnetic tuning of the scattering length across a complete range of positive and negative values. Experimental identification of the Feshbach resonance locations also assists accurate calculation of other cold collisional parameters (e.g., the triplet and singlet scattering lengths). In this paper we present measurements of the elastic cross section of $(3,-3)$ cesium atoms in a magnetic trap over the range of temperatures $(1-30$ μK) and in magnetic bias fields in the range (0.05 to 2.0 mT).

The principle of our experiment is to perturb the spatial and velocity distributions of atoms and measure the time taken for the atom cloud to relax back to equilibrium, as in Refs. [5,6]. We have used a TOP trap [25] with cylindrical symmetry about the *z* axis corresponding to the vertical direction in our apparatus. As in the original TOP trap experiments, atoms are removed which have a radial displacement from the *z* axis greater than the radius where the magnetic field is zero, or the radius where the applied rf induces transitions to other m_F states, which ever is less. Cutting in the radial direction causes an imbalance in the mean energy in the radial and axial directions $\overline{E_r}<\overline{E_z}$. In the subsequent reequilibriation, the size of the cloud in the axial *z* dimension must reduce relative to the radial *r* dimension. Monte Carlo (MC) simulations [5,6,24] show that the cloud aspect ratio *A* (the ratio of radial size to axial size) relaxes exponentially with time constant τ_a, thus $A-A_{\rm eq}=(A_0-A_{\rm eq})e^{-t/\tau_a}$, where $A_{\rm eq}$ is the equilibrium value and A_0 its initial value. The relaxation time τ_a is related to the average time between collisions in the cloud, τ_c by a factor $\tau_a=N_c\tau_c$, where N_c is a small number. In our experiment the density of the trapped atoms decreases with time because of trap losses caused by both two-body inelastic and background gas collisions. Inelastic collisions also lead to heating since the rate of inelastic collisions is highest at the bottom of the trap, where the density is high. Thus on average the lost atoms have less than average energy. However, the total energy of the trapped atoms rises by $<10\%$ of the initial energy during a rethermalization run, so in what follows we neglect this increase. From kinetic theory, the local collision rate is $R=n\sigma\overline{v}$ and the mean collision time $\tau_c=1/n\sigma\overline{v}$. At thermal

equilibrium, the velocity distribution is the same throughout the cloud so $\overline{n\sigma v}$ can be separated into the product of the mean density $\bar{n}$, defined as in Ref. [6] by $\bar{n} = \int n^2(\vec{r})d^3r / \int n(\vec{r})d^3r$ (this is $1/\sqrt{8}$ times the peak density for Gaussian distributions) and $\overline{\sigma v}$. σ is the elastic collision cross section and v is the atomic speed. Hence we have $\dot{A} = -(A - A_{\rm eq})\bar{n}(t)\overline{\sigma v}/N_c$ whose solution is

$$A(t) - A_{\rm eq} = (A_0 - A_{\rm eq}) \exp\left[- \frac{\overline{\sigma v}}{N_c} \int_0^t \bar{n}(t) dt \right]. \qquad (1)$$

We rewrite Eq. (1) as

$$A(t) - A_{\rm eq} = (A_0 - A_{\rm eq}) e^{-t_N/\tau_R}, \qquad (2)$$

where the ''renormalized time'' t_N is defined by $t_N = \int_0^t \bar{n}(t)/(\bar{n}_0) dt$, where $\bar{n}_0$ is the initial mean density and

$$\tau_R = N_c / \bar{n}_0 \overline{\sigma v}. \qquad (3)$$

Equation (2) then has the form of a simple exponential decay with respect to renormalized time t_N. This procedure rescales the time scale so that the relaxation curves are the same as one would obtain if the density remained constant.

A standard result [18] for the elastic cross section σ in the *s*-wave scattering regime in the presence of a zero-energy resonance is

$$\sigma = \frac{8\pi a^2}{1 + k^2 a^2}, \qquad (4)$$

where a is the *s*-wave scattering length and k is the magnitude of the relative wave vector of the colliding particles. From Eq. (4), one can identify two temperature regimes. In the first regime, defined by $ka \ll 1$, Eq. (4) simplifies to $\sigma = 8\pi a^2$ and N_c has been found from MC simulations [5,24] to be 2.7. Combining Eqs. (3) and (4) in this regime leads to the exact result $\sigma = 8\pi a^2 = 2.7/\bar{n}_0 \bar{v} \tau_R$, where $\bar{n}_0$, $\bar{v}$ and τ_R are all measurable, with $\bar{v} = 4(k_B T/\pi m)^{1/2}$ as in Ref. [6]. Thus σ and a can be determined in this regime. In the second regime, defined by $ka > 1$, Eq. (4) simplifies to $\sigma \simeq 8\pi/k^2$, i.e. $\sigma \propto 1/T$ and N_c is found from MC simulations [6] to be 10.5. This larger value arises because the collisions between faster atoms which are crucial for the redistribution of energy have a smaller cross section than for slower atoms.

We study the elastic cross section in a time-orbiting potential (TOP) trap [25], our version of which was previously described in Ref. [9]. To load the TOP trap, we first accumulate $\approx 2 \times 10^7$ cesium atoms in a dark SPOT trap [26]. The atoms are then optically pumped from the $F=3$ dark state to the bright (normal MOT) $F=4$ state, compressed for 20 ms in a 0.4 Tm^{-1} axial gradient, and sub-Doppler cooled in a 0.05 Tm^{-1} gradient for a further 20 ms. Within a few milliseconds, the cooled, compressed cloud is optically pumped back to the $F=3$ state, the 1 mT rotating bias field is switched on and the cloud is pumped into the $(F=3, m_F = -3)$ state. The (axial) quadrupole gradient is then switched to 1 Tm^{-1} in 1.5 ms, a value which gives good mode matching to the compressed MOT cloud. At this stage we typically have 5×10^6 atoms at ≈ 23 μK with a density of 3×10^9 cm^{-3} in the TOP trap. The trap stiffness is then adiabatically adjusted by changing the bias field B_t and axial quadrupole gradient B_q'. Finally the cloud is subjected to forced evaporative cooling by the ''circle of death'' [25] and an applied rf field to produce the temperature, density and bias field desired. Owing to the interplay between the trap stiffness $k(\propto B_q'^2/B_t)$ and the radius of the circle of death $(\propto B_t/B_q')$, the parameters of final temperature, final density and final bias field are not independent of each other. Nevertheless, a large volume of the parameter space can be accessed.

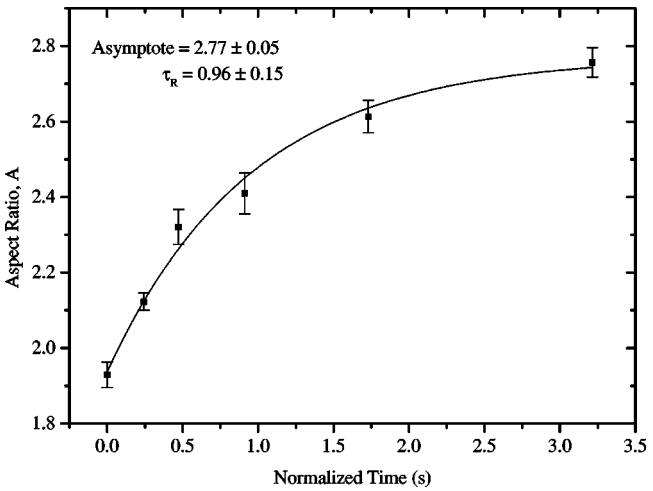

FIG. 1. A typical evolution of the aspect ratio plotted against normalized time, averaged over five runs. The error bars represent only the standard error χ of the five measurements averaged at each point. The solid line is a weighted fit of an exponential decay, the weight of each point being $1/\chi^2$.

To obtain a nonequilibrium distribution, the last stage of the forced rf evaporation (rf cutting) is carried out on a time scale (0.1 s) much shorter than the rethermalization time. The cut results in a cloud in which the ratio of the horizontal to vertical dimensions of the imaged cloud (aspect ratio) is less than its equilibrium value [28].

The cloud is then allowed to rethermalize for a variable equilibration time before being imaged by absorption shadow imaging. The probing sequence consists of two 10 μs pulses separated by 120 μs. The first pulse optically pumps the atoms from $(F, m_F) = (3, -3)$ to $(4, -4)$ and $(4, -3)$. The second pulse both optically pumps all the atoms into $(4, -4)$ and images them on the closed optical transition $(4, -4)$ to $(5', -5')$. The integrated cloud absorption have Gaussian profiles. From the measured $1/e$ sizes of the cloud and the total absorption, we calculate the temperature and density of the cloud (using the known trap potential). By repeating this procedure with an increasing series of equilibration times, the time constant τ_R, for relaxation of the cloud's aspect ratio is determined. Shot-to-shot variations are reduced by averaging the result of five loadings for each equilibration time. Typical results are shown in Fig. 1. Each

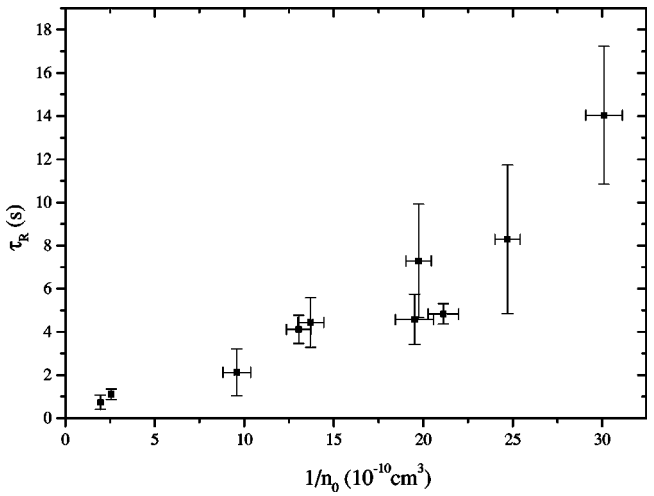

FIG. 2. Plot of τ_R against $1/\overline{n_0}$. Data taken at 6 μK and with $B_t = 0.6$ mT.

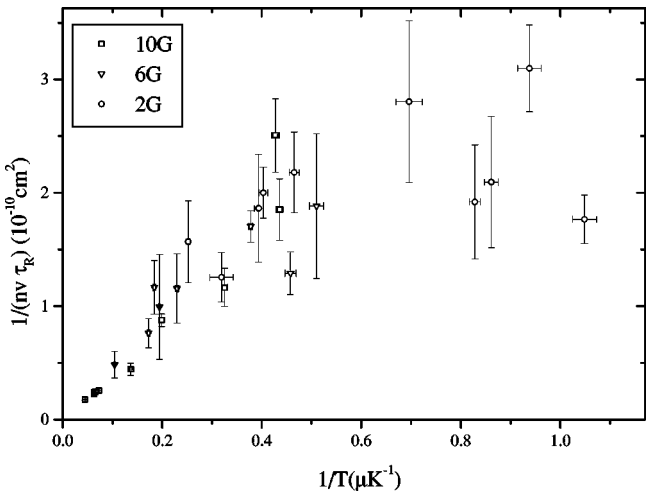

FIG. 4. Plot of $1/(\overline{n_0}\overline{v}\tau_R)$ against $1/T$. Circles: 0.2 mT, triangles: 0.6 mT, Squares: 1.0 mT.

rethermalization plot is fitted with an exponential decay to determine τ_R as defined by Eq. (2). The aspect ratio relaxes to a value in the range of 1.9 to 2.83 depending on the quadrupole field gradient B_q', and consistent with Ref. [28].

To confirm that the evolution of the aspect ratio was due to two-body collisions and not due to ergodic mixing in an anharmonic potential, we measured τ_R at various trap densities but at a fixed temperature of 6 ± 0.75 μK. The ergodic mixing rate is independent of density, whereas for collisional mixing, the time constant, τ_R is predicted [Eq. (3)] to vary inversely with density. Figure 2 is a plot of τ_R against $1/\overline{n_0}$ and the linearity of the plot confirms that the relaxation of the aspect ratio was due to elastic collisions.

We have measured τ_R over a range of temperatures from 1 to 30 μK and magnetic fields from 0.05 to 2.0 mT, endeavoring where possible to keep one of those two parameters fixed, while varying the other. The results are shown in Figs. 3 and 4, in the form of plots of $1/\overline{n_0}\overline{v}\tau_R$ against B_t and $1/T$, respectively.

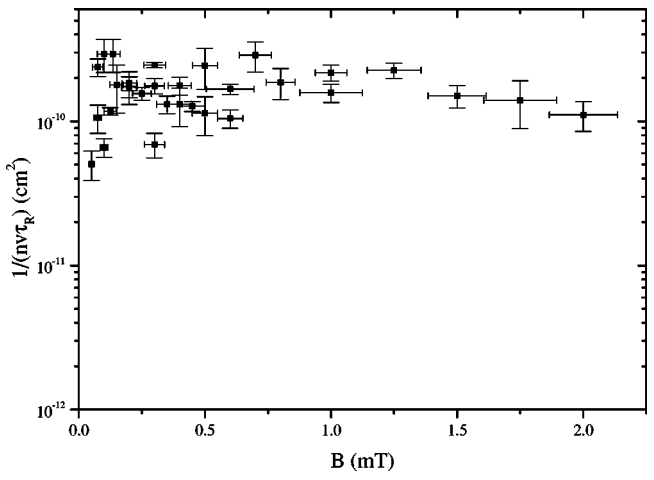

FIG. 3. Plot of $1/(\overline{n_0}\overline{v}\tau_R)$ against B_t. Data scaled to 2.7 μK using $1/T$ dependence shown in Fig. 4.

We initially assumed that τ_R would depend on both temperature T and bias field B_t, and we measured τ_R over as much of this two-dimensional parameter space as was experimentally accessible. However, we found that (within the limits set by the shot-to shot noise of our experiment) τ_R was essentially independent of B_t over the range studied (Fig. 3). We also found a marked temperature dependence (Fig. 4), which was independent of B_t. In the temperature range 3 to 30 μK, $1/(\overline{n_0}\overline{v}\tau_R)$ varies as $1/T$, but at lower T there is clear evidence of a saturation effect. This $1/T$ dependence and saturation is consistent with a zero-energy resonance, as described by Eq. (4) [29]. By multiplying the mean of the values of $1/(\overline{n_0}\overline{v}\tau_R)$ for the five lowest temperature points on Fig. 4 by the smallest N_c, i.e., 2.7, we can place a conservative lower bound on the magnitude of the scattering length for $(3,-3)$ s-wave collisions, and we find this to be $940a_0$ (Bohr radii). Error bars shown on all the graphs represent only the random statistical errors obtained during each experimental run and vary from ± 5 to $\pm 25\%$. The complete dataset was accumulated over many weeks, and additional random errors can be seen in the spread of data in Figs. 3 and 4. These additional errors are mainly due to day to day drifts in the absolute calibration of the measurement of the number of trapped atoms. The drifts are of order $\pm 10\%$ for larger clouds (obtained at high T and B_t) but increase up to $\pm 30\%$ for the smallest clouds measured (obtained at high T and B_t). Other significant errors included in our final error audit are imaging magnification ($\pm 5\%$), magnetic bias field and field gradient calibrations (± 5 and $\pm 7\%$); sources of error $< 5\%$ are neglected. Combining the above with the error bars already plotted for the values of $1/(\overline{n_0}\overline{v}\tau_R)$ in Figs. 3 and 4 leads to a final error varying from $\pm 17\%$ at high T, B_t to $\pm 35\%$ at low T, B_t. The error on the lower bound to the scattering length is half the error on $1/(\overline{n_0}\overline{v}\tau_R)$, but as we base our lower bound on a mean of five points, we quote this as -15%. Our result for the lower bound is consistent with results previously inferred from comparisons of evaporative cooling rates with a Monte Carlo simulation [10], from pho-

toassociation experiments [27] and from a recent measurement for $(3,+3)$ Cs atoms [12], but do not agree with a recent theoretical prediction [15], which suggests a lower value around $280a_0$, and also predicted a Feshbach resonance at a bias field around 0.1 mT. At the center of a Feshbach resonance the elastic cross section is expected to decrease by several orders of magnitude. In a magnetic trap, the atoms experience a range of bias fields, owing to the finite size of the cloud in the quadrupole gradient; the size of this spread is from 0.03 to 0.2 mT, as shown by the horizontal error bars in Fig. 3. This spreading would lead to a broadening of any resonance observed in our experiment, nevertheless one would still expect to observe a decrease in the measured elastic cross section of more than one order of magnitude at a resonance. The absence of such a decrease in our data rules out the existence of a Feshbach resonance in the range of B_t studied. Although we were able to run our TOP trap at fields as low as 0.02 mT, we were unable to explore the cross section in the regime below 0.05 mT as it was not possible to retain enough atoms (>5000) for well resolved imaging of the aspect ratio. Nor were we able to access the region of bias fields >2.5 mT, owing to the excessive heating of the magnetic field coils at those values.

In conclusion, we have observed the effect of a zero-energy resonance on the elastic scattering cross section of cesium atoms in the $F=3,m_F=-3$ state in a magnetic trap, and from this data, we deduce a lower bound for the scattering length of $940a_0$. We also find that the variation in the cross section with respect to magnetic bias field is less than $\pm 50\%$ over the range studied, which eliminates the existence for $(F=3,m_F=-3)$ scattering of a Feshbach resonance in this range (0.05 to 2.0 mT). The results are significant because they represent the largest observed elastic cross section amongst the alkali metals, and because they may allow more precise calculation of cesium collisional parameters, in turn allowing predictions of regimes favorable to Bose-Einstein condensation of cesium. The results are also relevant for attempts to trap the $F=3,m_F=+3$ high field seeking state, as the elastic cross section will be similarly large at low T. In regimes where the scattering length is negative, such a large magnitude may prevent the observation of stable condensates with a large number of atoms.

We would like to acknowledge helpful discussions with Paul Leo at N.I.S.T., and also thank Gerald Hechenblaikner for support. This work was supported by a grant from the EPSRC. O. Maragò acknowledges the support under TMR program, Grant No. ERBFMBICT 983077.

[1] M.H. Anderson *et al.*, Science **269**, 198 (1995).
[2] C.C. Bradley *et al.*, Phys. Rev. Lett. **75**, 1687 (1995).
[3] K.B. Davis *et al.*, Phys. Rev. Lett. **75**, 3969 (1995).
[4] D.G. Fried *et al.*, Phys. Rev. Lett. **81**, 3811 (1998).
[5] C.R. Monroe *et al.*, Phys. Rev. Lett. **70**, 414 (1993).
[6] M. Arndt *et al.*, Phys. Rev. Lett. **79**, 625 (1997).
[7] J. Söding *et al.*, Phys. Rev. Lett. **80**, 1869 (1998).
[8] P. Bance, Ph.D thesis, University of Oxford, 1998.
[9] J. Arlt *et al.*, J. Phys. B **31**, L321 (1998)
[10] D. Guéry-Odelin *et al.*, Opt. Express **2**, 323 (1998).
[11] D. Guéry-Odelin *et al.*, Europhys. Lett. **44**, 25 (1998).
[12] V. Vuletić *et al.*, Phys. Rev. Lett. **82**, 1406 (1999).
[13] E. Tiesinga, B.J. Verhaar, and H.T.C Stoof, Phys. Rev. A **47**, 4114 (1993).
[14] B.J. Verhaar, K. Gibble, and S. Chu, Phys. Rev. A **48**, R3429 (1993).
[15] S.J. Kokkelmans, B.J. Verhaar, and K. Gibble, Phys. Rev. Lett. **81**, 951 (1998).
[16] P.J. Leo *et al.*, Phys. Rev. Lett. **81**, 1389 (1998).
[17] R. Legere and K. Gibble, Phys. Rev. Lett. **81**, 5780 (1998).
[18] C.J. Joachim, *Quantum Collisions Theory* (North-Holland, Amsterdam, 1983).
[19] W. Ketterle and N.J. van Druten, Adv. At., Mol., Opt. Phys. **37**, 181 (1996).
[20] P. Leo and P. Julienne (Private communication).
[21] H. Feshbach, Ann. Phys. (N.Y.) **19**, 287 (1962).
[22] S. Inouye *et al.*, Nature (London) **392**, 151 (1998).
[23] J.L. Roberts *et al.*, Phys. Rev. Lett. **81**, 5109 (1998).
[24] H. Wu and C.J. Foot, J. Phys. B **29**, L321 (1996).
[25] W. Petrich *et al.*, Phys. Rev. Lett. **74**, 3352 (1995).
[26] W. Ketterle *et al.*, Phys. Rev. Lett. **70**, 2253 (1993).
[27] A. Fioretti *et al.*, Phys. Rev. Lett. **80**, 4402 (1998).
[28] The aspect ratio of the TOP trap varies as $\sqrt{8}[(x^2-1)/(x^2+1)]^{1/2}$, where $x=m_F g_F \mu_B B_q'/(mg)$ (J. Ensher, Ph.D thesis, University of Colorado, 1998).
[29] If one uses an alternative expression for σ such as Eq. (6) of Ref. [16], there is a third regime when $ka \gg 1$ and $kr_0 > 1$ where $\sigma \sim 1/T^2$. r_0 is the effective range of the potential. We do not see any $1/T^2$ dependence in our data, suggesting that our highest temperature points do not enter this regime, which in turn implies that $r_0 \leqslant 250a_0$.